

were used for the Debye temperatures, as were those of Vignos and Fairbank [in *Proceedings of the Eighth International Conference on Low-Temperature Physics, London, 1962*, edited by R. O. Davies (Butterworths, London, 1962)]. The ratio quoted in the text is rather

insensitive to the molar volume and was computed at a molar volume of 17.5 cm^3 .

¹⁸F. Y. Wu, H.-W. Lai, and C.-W. Woo, *J. Low Temp. Phys.* **3**, 331 (1970).

PHYSICAL REVIEW A

VOLUME 6, NUMBER 4

OCTOBER 1972

Experimental Electron Energy Distributions for Townsend Discharges in Argon Gas

Jon R. Losee and David S. Burch

Department of Physics, Oregon State University, Corvallis, Oregon 97331

(Received 16 August 1971; revised manuscript received 27 March 1972)

In this work the electron energy distribution functions and the anisotropic drift term of the velocity distribution functions in non-self-sustaining (Townsend) discharges in argon were determined by direct measurement for a range of E/N (electric field strength per gas-atom concentration) from 70 to 407 townsend (Td) ($1 \text{ Td} = 10^{-17} \text{ V cm}^2$). Some structure in the form of the distribution functions is observed, but the prediction of Heylen and Lewis for argon is not fully supported. The experimental method employed is to energy analyze electrons effusing from apertures in the anode of a discharge cell with a spherical retarding electric field. The experimental energy distributions were used along with cross-section data from the literature to compute the electron mobilities, diffusion constants, mean energies, and Townsend's first-ionization coefficients. Combination of the data with results from kinetic theory permitted evaluation of the anisotropic part of the velocity-distribution function.

INTRODUCTION

Gaseous discharges of the non-self-sustaining, or Townsend, type have a long history of service for investigation of the fundamental processes which occur when electrons pass through a gas of low concentration N . The electrons are driven by a uniform electric field E , and, over a wide range of the parameters, the behavior of the discharge is found to be governed by the quotient E/N . A complete description of Townsend discharges is afforded by a knowledge of the electron velocity distribution, which is also a function of E/N , and the cross sections for the various collisional processes available to the constituents of the discharge. In most cases, the electron-energy-distribution function serves as well as the velocity distribution for computation of the transport parameters.

Direct measurement of the important cross sections has been made for many gases, and transport parameters have been the object of most investigations which employed Townsend discharges. However, there has been but one prior report¹ of a direct measurement of the distribution functions. In this paper we present the results of further efforts, these to determine energy-distribution functions for Townsend discharges in argon.

EQUIPMENT AND DETAILS

The experimental method used in the present work is a modification of the retarding-field method

employed by Roberts and Burch.¹ The procedure will be discussed with reference to Fig. 1. Electrons effusing from apertures in the anode of the discharge cell are energy analyzed with a retarding electric field maintained between the anode and the collector. The anode of the discharge is a gold foil, $4.9 \mu\text{m}$ thick. It is perforated at its center with about 200 apertures of $13 \mu\text{m}$ diam and spaced $160 \mu\text{m}$ center to center in a circular area 2.5 mm in diam. A pattern of apertures is used rather than the large single aperture indicated in Fig. 1 so that adequate electron current to the collector can be realized along with satisfaction of the criterion for effusive flow. A guard ring,

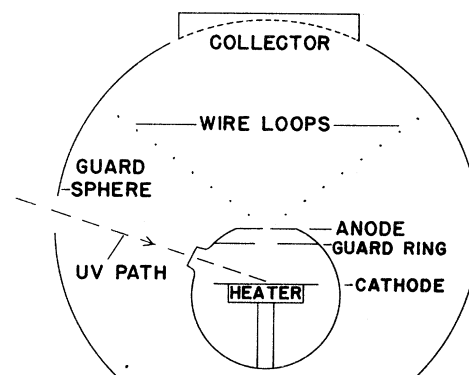


FIG. 1. Simplified schematic of the discharge cell and the energy analyzer.

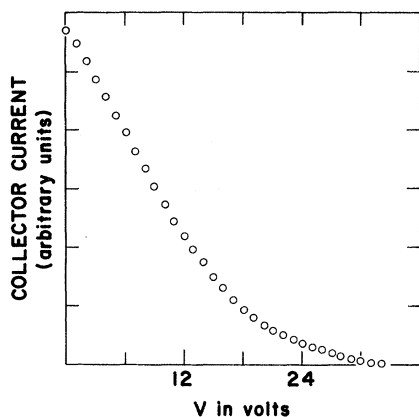


FIG. 2. Collector current vs retarding potential for $E/N=350$ Td.

1.5 in. o. d. and $\frac{3}{8}$ in. i. d. was placed 0.5 cm behind the anode to improve the uniformity of the discharge field in the central discharge region. It was operated at 75% of the anode-cathode potential difference. A nickel photocathode treated with activated oxides of barium and strontium was located 2 cm from the anode and was used along with a high-pressure Hg arc lamp to maintain the discharge. The discharge cell and all leads were electrostatically shielded from the retarding-field region. A cone of wire loops was installed in the guard sphere, each loop fixed at a potential such that a radial retarding field was approximated.

The gas used in the discharge cell was Matheson research-grade argon with a manufacturer's listed impurity of less than 3 ppm nitrogen. The gas pressure in the discharge cell ranged from 0.5 to 2 Torr, while the pressure in the retarding region was held to less than 10^{-5} Torr by a 6-in. oil diffusion pump. The only purification measure taken was to run the gas through a double liquid-nitrogen trap before it entered the cell.

The collector was a segment of the guard sphere, 4 in. across, centered on the axis of the discharge cell, and subtending a plane angle from this axis of 0.473 rad. This segment was a stainless-steel cup, 0.75 in. deep, covered with a spherically shaped stainless-steel screen. Both the cup and screen were platinum-blackened. The electron reflection characteristics of the collector were measured and found to be excellent and to have little energy dependence.² With a Townsend discharge current of the order of 10^{-9} A, a maximum collector current of about 5×10^{-14} A was observed and measured with a vibrating-reed electrometer.

DATA AND ANALYSIS

In this section, the raw data are discussed and the analysis leading to the energy-distribution

functions and to the anisotropic parts of the velocity-distribution functions is presented.

The data were collected in the form of measurements of the collector current as a function of retarding potential. Five measurements of the collector current at each retarding potential were obtained by alternating twice between successive retarding potentials spaced 1 V apart. Provided the five readings, normalized to constant discharge current, agreed to within 1%, they were averaged and recorded. Figure 2 shows the data of one run at $E/N=350$ Td.

To obtain the distribution function from the basic data, one needs an expression which relates it to the collector current. If the electron-velocity-distribution function in the gas-discharge cell is $f(\vec{v})$, then the flux P of electrons effusing from the pattern of apertures is, in spherical coordinates,

$$P = \int_0^\infty \int_0^{\theta_m} \int_0^{2\pi} f(v) v (\cos\theta) v^2 (\sin\theta) d\phi d\theta dv, \quad (1)$$

where θ_m is the angle subtended by the collector. For a cylindrically symmetric discharge, the velocity-distribution function can be expanded in Legendre polynomials. If the velocity-distribution function is not strongly peaked in the field direction, terms in the expansion of $f(\vec{v})$ of $P_2(\cos\theta)$ and higher can safely be dropped. With this approximation, the angular integrations in the expression for the electron flux can be performed. With $\theta_m = 0.473$ rad and the substitution $\epsilon = \frac{1}{2}mv^2$, the expression for the electron flux, in arbitrary units, becomes

$$P = \int_0^\infty [f_0(\epsilon) + 0.945f_1(\epsilon)] \epsilon d\epsilon. \quad (2)$$

In the determination of the collector current from the expression for the electron flux, two effects must be considered. First, the electrons are traveling in a retarding electric field after they leave the anode. If the experimental geometry was ideal, such that all electron paths were normal to the equipotential surfaces, the lower limit of the integral in Eq. (2), with ϵ in electron volts, would simply change from 0 to V , where V is the imposed retarding potential; however, since the anode is not a point source, and the retarding field is not perfectly radial, some electrons are deflected out of the cone subtended by the collector at the center of the anode. The departure from ideal geometry is accommodated by introducing a distortion function $D(V, \epsilon)$, defined to be the undeflected fraction of electrons of initial energy ϵ at retarding potential V ($\epsilon \geq V$). To determine the distortion function, a separate experiment was performed with the discharge cell evacuated. Careful analysis of measurements made without gas in the cell provided an approximate distortion function. The distortion function as determined without gas in the cell cannot be applied directly to the

gas case because of the difference in angular distribution of the electron flux in the two cases. To relate the two cases, a semiempirical distortion theory was developed which used approximate angular distributions for both cases and a simplified geometry for the retarding field. The development of the approximate distortion function is presented in the Appendix.

A second consideration in relating Eq. (2) to the measured collector current is that some of the electrons arriving at the collector with energy $(\epsilon - V)$ are reflected from that electrode and collected elsewhere. A second auxiliary experiment, employing a variable-energy electron gun, was performed to determine the total secondary-emission coefficient of the collector used.² If the collection efficiency of the collector is denoted by $T(\epsilon - V)$, the complete expression for the collector current, in arbitrary units, is

$$I(V) = \int_V^\infty [f_0(\epsilon) + 0.945f_1(\epsilon)]D(V, \epsilon)T(\epsilon - V)\epsilon d\epsilon. \quad (3)$$

The Boltzmann transport equation is now used to obtain a relationship between f_0 and f_1 . When $f_0(V) + f_1(V)\cos\theta$ is substituted into the Boltzmann transport equation for $f(V)$, there result two simultaneous equations for f_0 and f_1 . Under certain approximations,³ one of these equations gives the desired relationship:

$$f_1 = -\frac{E(df_0/d\epsilon)}{NQ_d + NQ_{in}}, \quad (4)$$

where E is the electric field intensity, Q_d is the diffusion (momentum transfer) cross section, and Q_{in} is the total inelastic cross section. This relationship, when used in Eq. (3), yields

$$I(V) = \int_V^\infty f_0 D(V, \epsilon) \epsilon T(\epsilon - V) d\epsilon - 0.945 \left(\frac{E}{N}\right) \int_V^\infty \frac{\epsilon D(V, \epsilon) T(\epsilon - V)}{(Q_d + Q_{in})} \frac{df_0}{d\epsilon} d\epsilon. \quad (5)$$

The second term can be integrated by parts; it becomes

$$+ 0.945 \left(\frac{E}{N}\right) \left[\frac{D(V, V)f_0(V)V}{Q_d(V) + Q_{in}(V)} + \int_V^\infty \frac{d}{d\epsilon} \left(\frac{\epsilon D(V, \epsilon) T(\epsilon - V)}{Q_d(\epsilon) + Q_{in}(\epsilon)} \right) f_0 d\epsilon \right].$$

In the evaluation, use has been made of the facts that $f_0(\epsilon)$ approaches zero rapidly at large ϵ and $T(0) = 1$.

Equation (5) can now be rearranged to give the integral equation for f_0 :

$$f_0(V) = \frac{Q_d(V) + Q_{in}(V)}{0.945(E/N)VD(V, V)}$$

$$\times \left\{ I(V) - \int_V^\infty f_0(\epsilon) \left[\epsilon D(V, \epsilon) T(\epsilon - V) + \frac{d}{d\epsilon} \left(\frac{\epsilon D(V, \epsilon) T(\epsilon - V)}{Q_d(\epsilon) + Q_{in}(\epsilon)} \right) \right] d\epsilon \right\}. \quad (6)$$

Finally, the energy-distribution function is given by

$$F_0(\epsilon) = \epsilon^{1/2} f_0(\epsilon) / \int_0^\infty \epsilon^{1/2} f_0(\epsilon) d\epsilon. \quad (7)$$

Also, $f_1(\epsilon)$ may be determined from f_0 and Eq. (4), and we define

$$F_1(\epsilon) = \epsilon^{1/2} f_1(\epsilon) / \int_0^\infty \epsilon^{1/2} f_0(\epsilon) d\epsilon. \quad (8)$$

RESULTS AND DISCUSSION

Equation (6) was solved numerically for f_0 by the following procedure: First, the trapezoidal rule was used to replace the integral by a sum, which was taken from V to 40 in 1-V steps. The sum was terminated at 40 since, for all data runs, $I(V)$ was negligible before 40-V retarding potential was reached. The integral equation is thus reduced to a set of simultaneous algebraic equations for the $f_0(V)$'s. The experimental data were entered as $I(V)$, $D(V, \epsilon)$, and $T(\epsilon - V)$ and the calculations were done with the aid of a CDC 3300 computer. Because the calculations were found to be relatively insensitive to the values of $Q_{in}(\epsilon)$, a reasonable extrapolation of the experimental findings of Maier-Leibnitz⁴ sufficed for our purposes. The diffusion cross section, on the other hand, presents a difficulty; reported values of $Q_d(\epsilon)$ are found to vary by as much as a factor of 2, and some of our results are quite sensitive to inaccuracies in this function. In the end, it was judged that the only reasonable procedure was to present our results twice, using two quite different functions for Q_d . The work of Graham and Ruhlig⁵ was taken as a reasonable estimate for the lower-limiting function, while the function as given by Massey, Burhop, and Gilbody⁶ served as an upper-limit estimate.

Figures 3 and 4 and Tables I and II give the final results for F_0 and F_1 . It is evident that the general shapes of these functions are not very sensitive to the choice of Q_d . Also, the energy distribution is in fair agreement with theoretical predictions of other workers.^{7,8} However, the sharp cutoff near the first excitation potential that appeared in the work of Heylen and Lewis⁹ is not observed in this experiment. Some structure in F_0 is evident at lower values of E/N , but it is only in the anisotropic part F_1 that structure appears consistently at about 11.5 and 15.5 eV, that is, at the onset energies for excitation and ionization. A dip in F_1 was frequently observed at around 5 eV; it is possible that this structure is due to small amounts

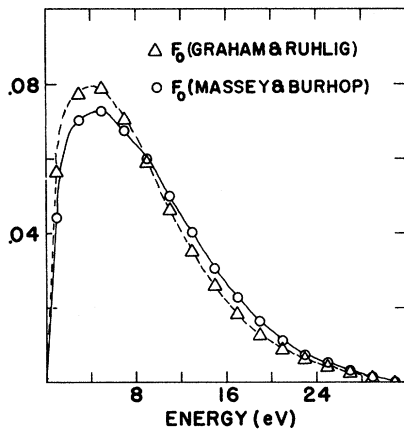


FIG. 3. Normalized energy distribution functions at $E/N = 282$ Td for both choices of the diffusion cross section.

of molecular impurity.

As may be seen from a development of Eq. (3), if $f_1(\epsilon)$ were either negligible or proportional to $f_0(\epsilon)$, and if $D(V, \epsilon)$ and $T(\epsilon - V)$ were both constant, as they would be for an ideal experimental apparatus, then F_0 could be found from

$$F_0(V) \propto -V^{-1/2} \frac{dI}{dV}. \quad (9)$$

This approximate relationship was often used during the course of the experiment to provide a simple analysis, and the sudden alterations in the slopes of curves of I vs V gave evidence that some structure in the distributions would be found in the full analysis.

In the development of the Boltzmann equation the assumption was made that the expansion of the

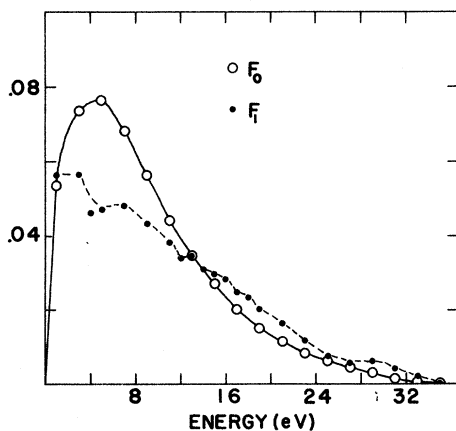


FIG. 4. Normalized distribution functions $F_0(\epsilon)$ and $F_1(\epsilon)$ at $E/N = 407$ Td for the Graham and Ruhlig diffusion cross section.

distribution function in Legendre polynomials is sufficiently convergent to permit neglect of terms in $P_2(\cos\theta)$ and higher orders. The validity of this assumption comes into question when one considers Fig. 4, which shows F_1 to be comparable to F_0 , and larger, in the tail. However, Fig. 4 is designed to show the extreme case, i. e., at the highest E/N and with use of the Graham-Ruhlig diffusion cross section. A study of Table II shows that, for all values of E/N studied, F_1 is found to be sensibly smaller than F_0 throughout the range of ϵ in which either is large if the Massey-Burhop-Gilbody values of Q_D are employed, and that the contribution from F_1 increases with increasing E/N . As Fig. 3 shows, the analysis for F_0 is rather insensitive to the choice of Q_D , and, indeed, F_0 is not altered drastically by leaving F_1 out of the analysis; we conclude that deletion of F_2 and higher-order terms is justified in the determination.

The cross sections and energy distributions were used to calculate the first Townsend coefficient α/N , the mobility $N\mu$, the diffusion coefficient ND , and the mean energy $\bar{\epsilon}$. The results are presented in Table III, where it can be seen that the choice of Q_d is critical. The ionization cross section of Rapp and Englander-Golden¹⁰ was employed in the computation of α/N , which is the only transport coefficient which has been measured in our range of E/N . Reference to Fig. 5 shows that the experimentally determined curve obtained by Kruithof and Penning¹¹ falls generally between the values we calculate from F_0 and our two choices of Q_d , the low values of Graham and Ruhlig⁵ giving

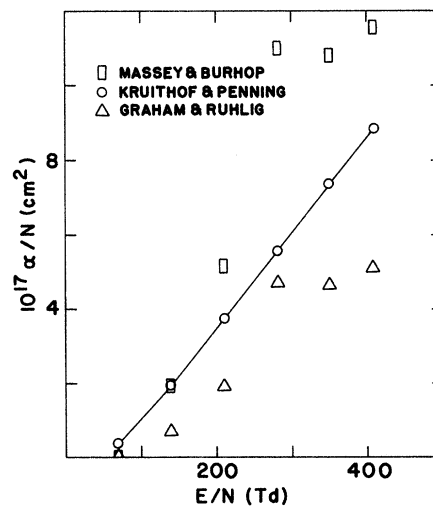


FIG. 5. The first Townsend coefficient as calculated from the energy distribution functions for both choices of the diffusion cross section compared to the experimental results of Kruithof and Penning.

correspondingly low values of α/N , while the cross section of Massey, Burhop, and Gilbody⁶ gives α/N larger than the experimental results. It seems probable, therefore, that Q_d lies between the two estimates we chose; the momentum transfer cross section for Ar as determined by Engelhardt and Phelps¹² is consistent with this conclusion.

The mobility and diffusion coefficient have been measured at low E/N only,^{12,13} but our results are not inconsistent with reasonable extrapolations from the measurements. Again, a more accurate knowledge of Q_d would be necessary for confident prediction of these transport quantities.

APPENDIX: DISTORTION FUNCTION

A perfect spherical analyzer with a monoenergetic point source, energy ϵ , would have constant

collector current I_0 at all retarding potentials $V < \epsilon$, and zero current for $V > \epsilon$. With distribution of energies, the ideal collector current $I_i(V, \epsilon)$ should saturate at $V = 0$. In an actual analyzer, the electron trajectories are not normal to equipotential surfaces at every point, and the collector current $I(V, \epsilon)$ is less than it would be for an ideal collector because the region near the source acts as a diverging lens. We define $D(V, \epsilon) = I(V, \epsilon)/I_i(V, \epsilon)$.

When the apparatus is operated with the discharge cell evacuated a strongly forward peaked beam of nearly monoenergetic electrons enters the analyzer. In this case, designated by subscript 0, the collector current at $V = 0$ is equal to the ideal collector current for $V < \epsilon$, i. e., $I_i(V, \epsilon) = I_0(0, \epsilon)$. Then, $D_0 = I_0(V, \epsilon)/I_0(0, \epsilon)$. Measurements made with our equipment revealed that

TABLE I. The experimental energy and anisotropic distributions for argon determined with use of the cross section given by Graham and Ruhlig. ϵ is in eV and F_0 and F_1 are in eV^{-1} .

E/N	70 Td		140 Td		210 Td		282 Td		350 Td		407 Td		
	ϵ	F_0	F_1										
0	0.0000	0.0000	0.0000	0.0000	0.0000	0.0000	0.0000	0.0000	0.0000	0.0000	0.0000	0.0000	0.0000
1	0.0870	0.0298	0.0618	0.0048	0.0605	0.0097	0.0563	0.0443	0.0542	0.0446	0.0537	0.0564	0.0564
2	0.1062	0.0245	0.0860	0.0139	0.0837	0.0268	0.0734	0.0411	0.0716	0.0470	0.0704	0.0570	0.0570
3	0.1026	0.0217	0.0933	0.0204	0.0872	0.0359	0.0774	0.0405	0.0755	0.0487	0.0737	0.0555	0.0555
4	0.1012	0.0208	0.0986	0.0220	0.0914	0.0326	0.0809	0.0355	0.0793	0.0431	0.0780	0.0461	0.0461
5	0.0836	0.0151	0.0946	0.0236	0.0870	0.0327	0.0790	0.0342	0.0771	0.0397	0.0765	0.0472	0.0472
6	0.0849	0.0098	0.0901	0.0231	0.0836	0.0285	0.0769	0.0338	0.0765	0.0386	0.0744	0.0479	0.0479
7	0.0723	0.0109	0.0807	0.0230	0.0772	0.0291	0.0707	0.0311	0.0704	0.0435	0.0681	0.0483	0.0483
8	0.0673	0.0068	0.0715	0.0214	0.0691	0.0291	0.0669	0.0310	0.0638	0.0407	0.0625	0.0445	0.0445
9	0.0635	0.0063	0.0625	0.0192	0.0612	0.0275	0.0591	0.0339	0.0578	0.0367	0.0564	0.0434	0.0434
10	0.0588	0.0052	0.0547	0.0167	0.0531	0.0250	0.0525	0.0303	0.0520	0.0350	0.0501	0.0420	0.0420
11	0.0572	0.0130	0.0481	0.0171	0.0467	0.0237	0.0463	0.0284	0.0463	0.0349	0.0441	0.0384	0.0384
12	0.0336	0.0112	0.0397	0.0180	0.0395	0.0217	0.0407	0.0271	0.0405	0.0321	0.0392	0.0341	0.0341
13	0.0374	0.0062	0.0323	0.0162	0.0347	0.0206	0.0353	0.0260	0.0361	0.0318	0.0349	0.0342	0.0342
14	0.0234	0.0161	0.0262	0.0151	0.0284	0.0221	0.0306	0.0242	0.0306	0.0308	0.0302	0.0312	0.0312
15	0.0088	0.0137	0.0200	0.0146	0.0229	0.0200	0.0261	0.0235	0.0268	0.0281	0.0271	0.0299	0.0299
16	0.0000	0.0054	0.0147	0.0138	0.0182	0.0162	0.0219	0.0212	0.0224	0.0265	0.0229	0.0288	0.0288
17		0.0000	0.0092	0.0113	0.0149	0.0156	0.0186	0.0185	0.0193	0.0229	0.0201	0.0250	0.0250
18			0.0064	0.0084	0.0109	0.0147	0.0158	0.0173	0.0164	0.0218	0.0173	0.0235	0.0235
19			0.0033	0.0086	0.0082	0.0119	0.0130	0.0154	0.0136	0.0201	0.0150	0.0203	0.0203
20			0.0004	0.0049	0.0056	0.0092	0.0110	0.0131	0.0114	0.0168	0.0131	0.0179	0.0179
21			0.0000	0.0007	0.0043	0.0057	0.0090	0.0115	0.0096	0.0118	0.0114	0.0164	0.0164
22				0.0000	0.0032	0.0058	0.0075	0.0088	0.0086	0.0093	0.0097	0.0153	0.0153
23					0.0018	0.0070	0.0063	0.0071	0.0074	0.0089	0.0083	0.0120	0.0120
24					0.0000	0.0038	0.0052	0.0060	0.0064	0.0083	0.0072	0.0083	0.0083
25						0.0000	0.0044	0.0057	0.0053	0.0065	0.0065	0.0077	0.0077
26							0.0033	0.0045	0.0047	0.0051	0.0054	0.0084	0.0084
27							0.0028	0.0037	0.0039	0.0063	0.0045	0.0060	0.0060
28							0.0019	0.0037	0.0028	0.0060	0.0040	0.0055	0.0055
29							0.0013	0.0033	0.0020	0.0048	0.0031	0.0061	0.0061
30							0.0006	0.0032	0.0013	0.0040	0.0023	0.0058	0.0058
31							0.0000	0.0014	0.0007	0.0030	0.0015	0.0043	0.0043
32								0.0000	0.0003	0.0020	0.0011	0.0028	0.0028
33									0.0000	0.0008	0.0006	0.0022	0.0022
34										0.0000	0.0004	0.0014	0.0014
35											0.0002	0.0007	0.0007
36											0.0003	0.0007	0.0007
37											0.0000	0.0008	0.0008
38												0.0000	0.0000

TABLE III. The transport parameters. The first set (upper) was calculated with use of the cross section given by Graham and Ruhlig and the second set (lower) was obtained from the cross section of Massey, Burhop, and Gilbody; $p\mu$ in $\text{cm}^2 \text{Torr}^{-1} \text{sec}^{-1}$, $N\mu$ in $\text{cm}^{-1} \text{v}^{-1} \text{sec}^{-1}$, pD in $\text{cm}^2 \text{Torr} \text{sec}^{-1}$, ND in $\text{cm}^{-1} \text{sec}^{-1}$, α/p in $\text{cm}^{-1}/\text{Torr}^{-1}$, α/N in cm^2 , and $\bar{\epsilon}$ and D/μ in eV.

E/N		$p\mu \times 10^{-5}$	$pD \times 10^{-6}$	α/p	D/μ	$N\mu \times 10^{-22}$	$ND \times 10^{-22}$	$\alpha/N \times 10^{17}$	$\bar{\epsilon}$	$(D/\mu)/\bar{\epsilon}^{-1}$
70	Td	4.23	1.83	0.00	4.32	1.50	6.46	0.00	6.17	0.699
140	Td	3.85	1.93	0.250	5.01	1.36	6.84	0.706	6.83	0.733
210	Td	3.97	2.08	0.687	5.24	1.41	7.37	1.94	7.37	0.711
282	Td	4.13	2.37	1.68	5.73	1.46	8.40	4.73	8.39	0.684
350	Td	4.12	2.45	1.66	5.95	1.45	8.67	4.68	8.66	0.687
407	Td	4.16	2.56	1.82	6.15	1.47	9.04	5.12	8.99	0.685
70	Td	3.12	1.77	0.00	5.65	1.105	6.25	0.00	6.52	0.867
140	Td	2.29	1.69	0.681	7.38	0.810	5.99	1.92	7.29	1.012
210	Td	2.24	1.70	1.80	7.57	0.794	6.00	5.07	8.03	0.942
282	Td	2.22	1.72	3.89	7.76	0.786	6.10	11.00	9.15	0.848
350	Td	2.16	1.73	3.82	8.01	0.766	6.13	10.80	9.47	0.846
407	Td	2.17	1.76	4.10	8.10	0.769	6.22	11.58	9.81	0.825

If we assume that $g(\theta)$ has the form $\cos^n \theta$, then measurements made with collectors of different diameter lead to the conclusion that $n \approx 8$ for electrons emerging from an evacuated cell. This distribution used in the model gives, to second order,

$$D_0(V, \epsilon) = 1 - 1.23k(V/\epsilon) + 1.05k^2(V/\epsilon)^2. \quad (\text{A2})$$

The corresponding expression for an isotropic source, such as is expected approximately to ob-

tain in the experiment, is

$$D(V, \epsilon) = 1 - 2k(V/\epsilon) + 3k^2(V/\epsilon)^2. \quad (\text{A3})$$

Comparison of (A2) with the experimental $D_0(V, \epsilon)$ led to

$$k \approx 0.118 + 0.304e^{-0.205\epsilon},$$

which was employed in (A3), the distortion function used for analysis of the experimental data.

¹T. D. Roberts and D. S. Burch, Phys. Rev. **142**, 100 (1966).

²J. R. Losee and D. S. Burch, Rev. Sci. Instr. **43**, 146 (1972).

³I. Abdelnabi and H. S. W. Massey, Proc. Phys. Soc. (London) **66**, 288 (1953).

⁴H. Maier-Leibnitz, Z. Physik **95**, 499 (1935).

⁵W. J. Graham and A. J. Ruhlig, Phys. Rev. **94**, 25 (1954).

⁶H. S. W. Massey, E. H. S. Burhop, and H. B. Gilbody, *Electronic and Ionic Impact Phenomena* (Clarendon, Oxford, England, 1969).

⁷V. E. Golant, Zh. Tekhn. Fiz. **4**, 680 (1959) [Sov. Phys. Tech. Phys. **29**, 756 (1959)].

⁸J. Fletcher and D. S. Burch (unpublished).

⁹A. E. D. Heylen and T. J. Lewis, Proc. Roy. Soc. (London) **271**, 531 (1963).

¹⁰D. Rapp and P. Englander-Golden, J. Chem. Phys. **43**, 1464 (1965).

¹¹A. A. Kruithof and F. M. Penning, Physica **3**, 515 (1936).

¹²A. G. Engelhardt and A. V. Phelps, Phys. Rev. **133**, 375 (1964).

¹³R. A. Nielsen, Phys. Rev. **50**, 950 (1936).